

# Outage Performance of Two-Way Relay Non-Orthogonal Multiple Access Systems

Xinwei Yue\*, Yuanwei Liu†, Shaoli Kang\*, Arumugam Nallanathan†, and Yue Chen†

\*Beihang University, Beijing, China

† Queen Mary University of London, London, UK

**Abstract**—This paper investigates a two-way relay non-orthogonal multiple access (TWR-NOMA) system, where two groups of NOMA users exchange messages with the aid of one half-duplex (HD) decode-and-forward (DF) relay. Since the signal-plus-interference-to-noise ratios (SINRs) of NOMA signals mainly depend on effective successive interference cancellation (SIC) schemes, imperfect SIC (ipSIC) and perfect SIC (pSIC) are taken into consideration. To characterize the performance of TWR-NOMA systems, we derive closed-form expressions for both exact and asymptotic outage probabilities of NOMA users' signals with ipSIC/pSIC. Based on the results derived, the diversity order and throughput of the system are examined. Numerical simulations demonstrate that: 1) TWR-NOMA is superior to TWR-OMA in terms of outage probability in low SNR regimes; and 2) Due to the impact of interference signal (IS) at the relay, error floors and throughput ceilings exist in outage probabilities and ergodic rates for TWR-NOMA, respectively.

## I. INTRODUCTION

With the purpose to meet the requirements of future radio access, the design of non-orthogonal multiple access (NOMA) technologies is important to enhance spectral efficiency and user access [1]. The major viewpoint of NOMA is to superpose multiple users by sharing radio resources (i.e., time/frequency/code) over different power levels [2–4]. Then the desired signals are detected by exploiting the successive interference cancellation (SIC) [5]. Very recently, the integration of cooperative communication with NOMA has been widely discussed in many treaties [6–9]. Cooperative NOMA has been proposed in [6], where the user with better channel condition acts as a decode-and-forward (DF) relay to forward information. With the objective of improving energy efficiency, the application of simultaneous wireless information and power transfer (SWIPT) to the nearby user was investigated where the locations of NOMA users were modeled by stochastic geometry [7]. Considering the impact of imperfect channel state information (CSI), the authors in [8] investigated the performance of amplify-and-forward (AF) relay for downlink NOMA networks, where the exact and tight bounds of outage probability were derived. To further enhance spectrum efficiency, the performance of full-duplex (FD) cooperative NOMA was characterized in terms of outage behaviors [9], where user relaying was capable of switching operation between FD and HD mode.

Above existing treaties on cooperative NOMA are all based on one-way relay scheme, where the messages are delivered in only one direction, (i.e., from the BS to the relay or user destinations). As a further advance, two-way relay (TWR)

technique introduced in [10] has attracted remarkable interest as it is capable of boosting spectral efficiency. The basic idea of TWR systems is to exchange information between two nodes with the help of a relay. In [11], the authors studied the outage behaviors of DF relay with perfect and imperfect CSI conditions. In terms of CSI and system state information (SSI), the system outage behavior was investigated for two-way full-duplex (FD) DF relay on different multi-user scheduling schemes [12].

Motivated by the above two technologies, we focus our attentions on the outage behaviors of TWR-NOMA systems, where two groups of NOMA users exchange messages with the aid of a relay node using DF protocol. Considering both perfect SIC (pSIC) and imperfect SIC (ipSIC), we derive the closed-form expressions of outage probabilities for users' signals. To provide valuable insights, we further derive the asymptotic outage probabilities of users' signals and obtain the diversity orders. We show that the outage performance of TWR-NOMA is superior to TWR-OMA in the low signal-to-noise ratio (SNR) regime. We demonstrate that the outage probabilities for TWR-NOMA converge to error floors due to the effect of interference signal (IS) at the relay. We confirm that the use of pSIC is incapable of overcoming the zero diversity order for TWR-NOMA. Additionally, we discuss the system throughput in delay-limited transmission mode.

## II. SYSTEM MODEL

We consider a two-way relay NOMA communication scenario which consists of one relay  $R$ , two pairs of NOMA users  $G_1 = \{D_1, D_2\}$  and  $G_2 = \{D_3, D_4\}$ . Assuming that  $D_1$  and  $D_3$  are the nearby users in group  $G_1$  and  $G_2$ , respectively, while  $D_2$  and  $D_4$  are the distant users in group  $G_1$  and  $G_2$ , respectively. The exchange of information between user groups  $G_1$  and  $G_2$  is facilitated via the assistance of a decode-and-forward (DF) relay with two antennas, namely  $A_1$  and  $A_2$ . User nodes are equipped with single antenna and can transmit the superposed signals [13, 14]. In addition, we assume that the direct links between two pairs of users are inexistent due to the effect of strong shadowing. Without loss of generality, all the wireless channels are modeled to be independent quasi-static block Rayleigh fading channels and disturbed by additive white Gaussian noise with mean power  $N_0$ . We denote that  $h_1, h_2, h_3$  and  $h_4$  are denoted as the complex channel coefficient of  $D_1 \leftrightarrow R, D_2 \leftrightarrow R, D_3 \leftrightarrow R$  and  $D_4 \leftrightarrow R$  links, respectively. The channel power gains

$|h_1|^2$ ,  $|h_2|^2$ ,  $|h_3|^2$  and  $|h_4|^2$  are assumed to be exponentially distributed random variables (RVs) with the parameters  $\Omega_i$ ,  $i \in \{1, 2, 3, 4\}$ , respectively. It is assumed that the perfect CSIs of NOMA users are available at  $R$  for signal detection.

During the first slot, the pair of NOMA users in  $G_1$  transmit the signals to  $R$  just as uplink NOMA. Due to  $R$  is equipped with two antennas, when the  $R$  receives the signals from the pair of users in  $G_1$ , it will suffer from interference signals from the pair of users in  $G_2$ . More precisely, the observation at  $R$  for  $A_1$  is given by

$$y_{R_{A_1}} = h_1\sqrt{a_1P_u}x_1 + h_2\sqrt{a_2P_u}x_2 + \varpi_1I_{R_{A_2}} + n_{R_{A_1}}, \quad (1)$$

where  $I_{R_{A_2}}$  denotes IS from  $A_2$  with  $I_{R_{A_2}} = (h_3\sqrt{a_3P_u}x_3 + h_4\sqrt{a_4P_u}x_4)$ .  $\varpi_1 \in [0, 1]$  denotes the impact levels of IS at  $R$ .  $P_u$  is the normalized transmission power at user nodes.  $x_1$ ,  $x_2$  and  $x_3$ ,  $x_4$  are the signals of  $D_1$ ,  $D_2$  and  $D_3$ ,  $D_4$ , respectively, i.e.,  $\mathbb{E}\{x_1^2\} = \mathbb{E}\{x_2^2\} = \mathbb{E}\{x_3^2\} = \mathbb{E}\{x_4^2\} = 1$ .  $a_1$ ,  $a_2$  and  $a_3$ ,  $a_4$  are the corresponding power allocation coefficients. Note that the efficient uplink power control is capable of enhancing the performance of the systems considered, which is beyond the scope of this paper.  $n_{R_{A_j}}$  denotes the Gaussian noise at  $R$  for  $A_j$ ,  $j \in \{1, 2\}$ .

Similarly, when  $R$  receives the signals from the pair of users in  $G_2$ , it will suffer from interference signals from the pair of users in  $G_1$  as well and then the observation at  $R$  is given by

$$y_{R_{A_2}} = h_3\sqrt{a_3P_u}x_3 + h_4\sqrt{a_4P_u}x_4 + \varpi_1I_{R_{A_1}} + n_{R_{A_2}}, \quad (2)$$

where  $I_{R_{A_1}}$  denotes the interference signals from  $A_1$  with  $I_{R_{A_1}} = (h_1\sqrt{a_1P_u}x_1 + h_2\sqrt{a_2P_u}x_2)$ .

Applying the NOMA protocol,  $R$  first decodes  $D_l$ 's information  $x_l$  by the virtue of treating  $x_t$  as IS. Hence the received signal-to-interference-plus-noise ratio (SINR) at  $R$  to detect  $x_l$  is given by

$$\gamma_{R \rightarrow x_l} = \frac{\rho|h_l|^2a_l}{\rho|h_t|^2a_t + \rho\varpi_1(|h_k|^2a_k + |h_r|^2a_r) + 1}, \quad (3)$$

where  $\rho = \frac{P_u}{N_0}$  denotes the transmit signal-to-noise ratio (SNR),  $(l, k) \in \{(1, 3), (3, 1)\}$ ,  $(t, r) \in \{(2, 4), (4, 2)\}$ .

After SIC is carried out at  $R$  for detecting  $x_l$ , the received SINR at  $R$  to detect  $x_t$  is given by

$$\gamma_{R \rightarrow x_t} = \frac{\rho|h_t|^2a_t}{\varepsilon\rho|g|^2 + \rho\varpi_1(|h_k|^2a_k + |h_r|^2a_r) + 1}, \quad (4)$$

where  $\varepsilon = 0$  and  $\varepsilon = 1$  denote the pSIC and ipSIC employed at  $R$ , respectively. Due to the impact of ipSIC, the residual IS is modeled as Rayleigh fading channels [15] denoted as  $g$  with zero mean and variance  $\Omega_I$ .

In the second slot, the information is exchanged between  $G_1$  and  $G_2$  by the virtue of  $R$ . Therefore, just like the downlink NOMA,  $R$  transmits the superposed signals  $(\sqrt{b_1P_r}x_1 + \sqrt{b_2P_r}x_2)$  and  $(\sqrt{b_3P_r}x_3 + \sqrt{b_4P_r}x_4)$  to  $G_2$  and  $G_1$  by  $A_2$  and  $A_1$ , respectively.  $b_1$  and  $b_2$  denote the power allocation coefficients of  $D_1$  and  $D_2$ , while  $b_3$  and  $b_4$

are the corresponding power allocation coefficients of  $D_3$  and  $D_4$ , respectively.  $P_r$  is the normalized transmission power at  $R$ . In particular, to ensure the fairness between users in  $G_1$  and  $G_2$ , a higher power should be allocated to the distant user who has the worse channel conditions. Hence we assume that  $b_2 > b_1$  with  $b_1 + b_2 = 1$  and  $b_4 > b_3$  with  $b_3 + b_4 = 1$ . Note that the fixed power allocation coefficients for two groups' NOMA users are considered. Relaxing this assumption will further improve the performance of systems and should be concluded in our future work.

According to NOMA protocol, SIC is employed and the received SINR at  $D_k$  to detect  $x_t$  is given by

$$\gamma_{D_k \rightarrow x_t} = \frac{\rho|h_k|^2b_t}{\rho|h_k|^2b_l + \rho\varpi_2|h_k|^2 + 1}, \quad (5)$$

where  $\varpi_2 \in [0, 1]$  denotes the impact level of IS at the user nodes. Then  $D_k$  detects  $x_l$  and gives the corresponding SINR as follows:

$$\gamma_{D_k \rightarrow x_l} = \frac{\rho|h_k|^2b_l}{\varepsilon\rho|g|^2 + \rho\varpi_2|h_k|^2 + 1}. \quad (6)$$

Furthermore, the received SINR at  $D_t$  to detect  $x_r$  is given by

$$\gamma_{D_r \rightarrow x_t} = \frac{\rho|h_r|^2b_t}{\rho|h_r|^2b_l + \rho\varpi_2|h_r|^2 + 1}. \quad (7)$$

From above process, the exchange of information is achieved between the NOMA users for  $G_1$  and  $G_2$ .

### III. OUTAGE PROBABILITY

In this section, the performance of TWR-NOMA is characterized in terms of outage probability.

1) *Outage Probability of  $x_l$* : In TWR-NOMA, the outage events of  $x_l$  are explained as follow: i)  $R$  cannot decode  $x_l$  correctly; ii) The information  $x_t$  cannot be detected by  $D_k$ ; and iii)  $D_k$  cannot detect  $x_l$ , while  $D_k$  can first decode  $x_t$  successfully. To simplify the analysis, the complementary events of  $x_l$  are employed to express its outage probability. Hence the outage probability of  $x_l$  with ipSIC for TWR-NOMA is expressed as

$$P_{x_l}^{ipSIC} = 1 - \Pr(\gamma_{R \rightarrow x_l} > \gamma_{th_l}) \times \Pr(\gamma_{D_k \rightarrow x_t} > \gamma_{th_t}, \gamma_{D_k \rightarrow x_l} > \gamma_{th_l}), \quad (8)$$

where  $\varepsilon = 1$ ,  $\varpi_1 \in [0, 1]$  and  $\varpi_2 \in [0, 1]$ .  $\gamma_{th_l} = 2^{2R_l} - 1$  with  $R_l$  being the target rate at  $D_k$  to detect  $x_l$  and  $\gamma_{th_t} = 2^{2R_t} - 1$  with  $R_t$  being the target rate at  $D_k$  to detect  $x_t$ .

The following theorem provides the outage probability of  $x_l$  for TWR-NOMA.

**Theorem 1.** *The closed-form expression for the outage probability of  $x_l$  for TWR-NOMA with ipSIC is given by*

$$P_{x_l}^{ipSIC} = 1 - e^{-\frac{\beta_l}{\Omega_l}} \prod_{i=1}^3 \lambda_i \left( \frac{\Phi_1 \Omega_l}{\Omega_l \lambda_1 + \beta_l} - \frac{\Phi_2 \Omega_l}{\Omega_l \lambda_2 + \beta_l} + \frac{\Phi_3 \Omega_l}{\Omega_l \lambda_3 + \beta_l} \right) \left( e^{-\frac{\theta_l}{\Omega_k}} - \frac{\varepsilon \tau_l \rho \Omega_I}{\Omega_k + \varepsilon \rho \tau_l \Omega_I} e^{-\frac{\theta_l (\Omega_k + \varepsilon \rho \tau_l \Omega_I)}{\varepsilon \tau_l \rho \Omega_I \Omega_k} + \frac{1}{\varepsilon \rho \Omega_I}} \right), \quad (9)$$

where  $\varepsilon = 1$ ,  $\lambda_1 = \frac{1}{\rho a_t \Omega_t}$ ,  $\lambda_2 = \frac{1}{\rho \varpi_1 a_k \Omega_k}$  and  $\lambda_3 = \frac{1}{\rho \varpi_1 a_r \Omega_r}$ .  
 $\beta_l = \frac{\gamma_{th_l}}{\rho a_t}$ ,  $\Phi_1 = \frac{1}{(\lambda_2 - \lambda_1)(\lambda_3 - \lambda_1)}$ ,  $\Phi_2 = \frac{1}{(\lambda_3 - \lambda_2)(\lambda_2 - \lambda_1)}$  and  
 $\Phi_3 = \frac{1}{(\lambda_3 - \lambda_1)(\lambda_3 - \lambda_2)}$ .  $\theta_l \triangleq \max(\tau_l, \xi_t)$ .  $\tau_l = \frac{\gamma_{th_l}}{\rho(b_l - \varpi_2 \gamma_{th_l})}$   
with  $b_l > \varpi_2 \gamma_{th_l}$  and  $\xi_t = \frac{\gamma_{th_t}}{\rho(b_t - b_l \gamma_{th_t} - \varpi_2 \gamma_{th_t})}$  with  
 $b_t > (b_l + \varpi_2) \gamma_{th_t}$ .

*Proof.* See Appendix A.  $\square$

**Corollary 1.** Based on (9), for the special case  $\varepsilon = 0$ , the outage probability of  $x_1$  for TWR-NOMA with pSIC is given by

$$P_{x_1}^{pSIC} = 1 - e^{-\frac{\beta_l}{\Omega_t} - \frac{\theta_l}{\Omega_k}} \prod_{i=1}^3 \lambda_i \left( \frac{\Phi_1 \Omega_l}{\Omega_l \lambda_1 + \beta_l} - \frac{\Phi_2 \Omega_l}{\Omega_l \lambda_2 + \beta_l} + \frac{\Phi_3 \Omega_l}{\Omega_l \lambda_3 + \beta_l} \right). \quad (10)$$

2) *Outage Probability of  $x_t$ :* Based on NOMA principle, the complementary events of outage for  $x_t$  have the following cases. One of the cases is that  $R$  can first decode the information  $x_l$  and then detect  $x_t$ . Another case is that either of  $D_k$  and  $D_r$  can detect  $x_t$  successfully. Hence the outage probability of  $x_t$  can be expressed as

$$P_{x_t}^{ipSIC} = 1 - \Pr(\gamma_{R \rightarrow x_t} > \gamma_{th_t}, \gamma_{R \rightarrow x_l} > \gamma_{th_l}) \times \Pr(\gamma_{D_k \rightarrow x_t} > \gamma_{th_t}) \Pr(\gamma_{D_r \rightarrow x_t} > \gamma_{th_t}), \quad (11)$$

where  $\varepsilon = 1$ ,  $\varpi_1 \in [0, 1]$  and  $\varpi_2 \in [0, 1]$ .

The following theorem provides the outage probability of  $x_t$  for TWR-NOMA.

**Theorem 2.** The closed-form expression for the outage probability of  $x_t$  with ipSIC is given by

$$P_{x_t}^{ipSIC} = 1 - \frac{e^{-\frac{\beta_l}{\Omega_t} - \beta_t \varphi_t - \frac{\xi}{\Omega_k} - \frac{\xi}{\Omega_r}}}{\varphi_t \Omega_t (1 + \varepsilon \beta_t \rho \varphi_t \Omega_I) (\lambda'_2 - \lambda'_1)} \prod_{i=1}^2 \lambda'_i \times \left( \frac{\Omega_l}{\beta_l + \beta_t \Omega_1 \varphi_t + \Omega_l \lambda'_1} - \frac{\Omega_l}{\beta_l + \beta_t \Omega_1 \varphi_t + \Omega_l \lambda'_2} \right), \quad (12)$$

where  $\varepsilon = 1$ ,  $\lambda'_1 = \frac{1}{\rho \varpi_1 a_k \Omega_k}$  and  $\lambda'_2 = \frac{1}{\rho \varpi_1 a_r \Omega_r}$ .  $\beta_t = \frac{\gamma_{th_t}}{\rho a_t}$ ,  $\varphi_t = \frac{\Omega_l + \rho \beta_l a_t \Omega_t}{\Omega_l \Omega_t}$ .

*Proof.* See Appendix B.  $\square$

**Corollary 2.** For the special case, substituting  $\varepsilon = 0$  into (12), the outage probability of  $x_2$  for TWR-NOMA with pSIC is given by

$$P_{x_t}^{pSIC} = 1 - \frac{e^{-\frac{\beta_l}{\Omega_t} - \beta_t \varphi_t - \frac{\xi}{\Omega_k} - \frac{\xi}{\Omega_r}}}{\varphi_t \Omega_t (\lambda'_2 - \lambda'_1)} \prod_{i=1}^2 \lambda'_i \times \left( \frac{\Omega_l}{\beta_l + \beta_t \Omega_1 \varphi_t + \Omega_l \lambda'_1} - \frac{\Omega_l}{\beta_l + \beta_t \Omega_1 \varphi_t + \Omega_l \lambda'_2} \right). \quad (13)$$

3) *Diversity Order Analysis:* To obtain deeper insights for TWR-NOMA systems, the asymptotic analysis are presented in high SNR regimes based on the derived outage probabilities. The diversity order is defined as [16, 17]

$$d = - \lim_{\rho \rightarrow \infty} \frac{\log(P_{x_i}^{\infty}(\rho))}{\log \rho}, \quad (14)$$

where  $P_{x_i}^{\infty}$  denotes the asymptotic outage probability of  $x_i$ .

**Proposition 1.** Based on the analytical results in (9) and (10), when  $\rho \rightarrow \infty$ , the asymptotic outage probabilities of  $x_l$  for ipSIC/pSIC with  $e^{-x} \approx 1 - x$  are given by

$$P_{x_l, \infty}^{ipSIC} = 1 - \prod_{i=1}^3 \lambda_i \left( \frac{\Phi_1 \Omega_l}{\Omega_l \lambda_1 + \beta_l} - \frac{\Phi_2 \Omega_l}{\Omega_l \lambda_2 + \beta_l} + \frac{\Phi_3 \Omega_l}{\Omega_l \lambda_3 + \beta_l} \right) \times \left[ 1 - \frac{\theta_l}{\Omega_k} - \frac{\varepsilon \tau \rho \Omega_I}{\Omega_k + \varepsilon \tau \rho \Omega_I} \left( 1 - \frac{\theta_l (\Omega_k + \varepsilon \tau \rho \Omega_I)}{\tau \varepsilon \rho \Omega_I \Omega_k} \right) \right], \quad (15)$$

and

$$P_{x_l, \infty}^{pSIC} = 1 - \prod_{i=1}^3 \lambda_i \left( \frac{\Phi_1 \Omega_l}{\Omega_l \lambda_1 + \beta_l} - \frac{\Phi_2 \Omega_l}{\Omega_l \lambda_2 + \beta_l} + \frac{\Phi_3 \Omega_l}{\Omega_l \lambda_3 + \beta_l} \right), \quad (16)$$

respectively. Substituting (15) and (16) into (14), the diversity orders of  $x_l$  with ipSIC/pSIC are equal to zeros.

**Remark 1.** An important conclusion from above analysis is that due to impact of residual interference, the diversity order of  $x_l$  with the use of ipSIC is zero. Additionally, the communication process of the first slot similar to uplink NOMA, even though under the condition of pSIC, diversity order is equal to zero as well for  $x_l$ . As can be observed that there are error floors for  $x_l$  with ipSIC/pSIC.

**Proposition 2.** Similar to the resolving process of (15) and (16), the asymptotic outage probabilities of  $x_t$  with ipSIC/pSIC in high SNR regimes are given by

$$P_{x_t, \infty}^{ipSIC} = 1 - \frac{\lambda'_1 \lambda'_2}{\varphi_t \Omega_t (1 + \varepsilon \rho \beta_t \varphi_t \Omega_I) (\lambda'_2 - \lambda'_1)} \times \left( \frac{\Omega_l}{\beta_l + \beta_t \Omega_1 \varphi_t + \Omega_l \lambda'_1} - \frac{\Omega_l}{\beta_l + \beta_t \Omega_1 \varphi_t + \Omega_l \lambda'_2} \right), \quad (17)$$

and

$$P_{x_t, \infty}^{pSIC} = 1 - \frac{\lambda'_1 \lambda'_2}{\varphi_t \Omega_t (\lambda'_2 - \lambda'_1)} \times \left( \frac{\Omega_l}{\beta_l + \beta_t \Omega_1 \varphi_t + \Omega_l \lambda'_1} - \frac{\Omega_l}{\beta_l + \beta_t \Omega_1 \varphi_t + \Omega_l \lambda'_2} \right), \quad (18)$$

respectively. Substituting (17) and (18) into (14), the diversity orders of  $x_t$  for both ipSIC and pSIC are zeros.

**Remark 2.** Based on above analytical results of  $x_l$ , the diversity orders of  $x_t$  with ipSIC/pSIC are also equal to zeros. This is because residual interference is existent in the total communication process.

TABLE I: Table of Parameters for Numerical Results

Monte Carlo simulations repeated	$10^6$ iterations
Power allocation coefficients of NOMA	$b_1 = b_3 = 0.2$ $b_2 = b_4 = 0.8$
Targeted data rates	$R_1 = R_3 = 0.1$ BPCU $R_2 = R_4 = 0.01$ BPCU
Pass loss exponent	$\alpha = 2$
The distance between R and $D_1$ or $D_3$	$d_1 = 2$ m
The distance between R and $D_2$ or $D_4$	$d_2 = 10$ m

4) *Throughput Analysis*: In delay-limited transmission scenario, the BS transmits message to users at a fixed rate, where system throughput will be subject to wireless fading channels. Hence the corresponding throughput of TWR-NOMA with ipSIC/pSIC is calculated as [7]

$$R_{dl}^{\psi} = (1 - P_{x_1}^{\psi}) R_{x_1} + (1 - P_{x_2}^{\psi}) R_{x_2} + (1 - P_{x_3}^{\psi}) R_{x_3} + (1 - P_{x_4}^{\psi}) R_{x_4}, \quad (19)$$

where  $\psi \in (ipSIC, pSIC)$ .  $P_{x_1}^{\psi}$  and  $P_{x_3}^{\psi}$  with ipSIC/pSIC can be obtained from (9) and (10), respectively, while  $P_{x_2}^{\psi}$  and  $P_{x_4}^{\psi}$  with ipSIC/pSIC can be obtained from (12) and (13), respectively.

#### IV. NUMERICAL RESULTS

In this section, numerical results are provide to investigate the impact levels of IS on outage probability for TWR-NOMA systems. The simulation parameters used are summarized in Table I, where BPCU is short for bit per channel use. Due to the reciprocity of channels between  $G_1$  and  $G_2$ , the outage behaviors of  $x_1$  and  $x_2$  in  $G_1$  are presented to illustrate availability of TWR-NOMA. Without loss of generality, the power allocation coefficients of  $x_1$  and  $x_2$  are set as  $a_1 = 0.8$  and  $a_2 = 0.2$ , respectively.  $\Omega_1$  and  $\Omega_2$  are set to be  $\Omega_1 = d_1^{-\alpha}$  and  $\Omega_2 = d_2^{-\alpha}$ , respectively.

##### A. Outage Probability

Fig. 1 plots the outage probabilities of  $x_1$  and  $x_2$  with both ipSIC and pSIC versus SNR for simulation setting with  $\varpi_1 = \varpi_2 = 0.01$  and  $\Omega_I = -20$  dB. The solid and dashed curves represent the exact theoretical performance of  $x_1$  and  $x_2$  for both ipSIC and pSIC, corresponding to the results derived in (9), (10) and (12), (13), respectively. Apparently, the outage probability curves match perfectly with Monte Carlo simulation results. As can be observed from the figure, the outage behaviors of  $x_1$  and  $x_2$  for TWR-NOMA are superior to TWR-OMA in the low SNR regime. This is due to the fact that the influence of IS is not the dominant factor at low SNR. Furthermore, another observation is that the pSIC is capable of enhancing the performance of NOMA compare to the ipSIC. In addition, the asymptotic curves of  $x_1$  and  $x_2$  with ipSIC/pSIC are plotted according to (15), (16) and (17), (16), respectively. It can be seen that the outage behaviors of  $x_1$  and  $x_2$  converge to the error floors in the high SNR regime. The reason can be explained that due to the impact of residual interference by the use of ipSIC,  $x_1$  and  $x_2$  result in zero diversity orders. Although the pSIC is carried out in

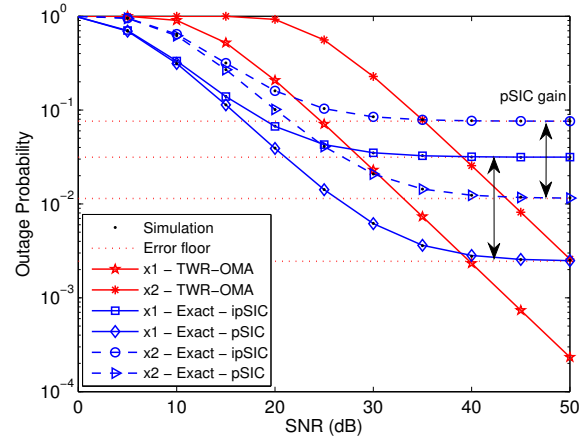
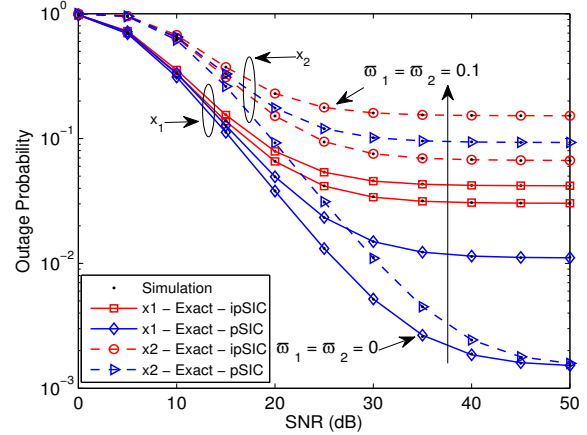


Fig. 1: Outage probability versus the transmit SNR.


 Fig. 2: Outage probability versus the transmit SNR, with  $\Omega_I = -20$  dB.

TWR-NOMA system,  $x_1$  and  $x_2$  also obtain zero diversity orders. This is due to the fact that when the relay first detect the strongest signal in the first slot, it will suffer interference from the weaker signal. This observation verifies the conclusion **Remark 1** in Section III.

Fig. 2 plots the outage probabilities of  $x_1$  and  $x_2$  versus SNR with the different impact levels of IS from  $\varpi_1 = \varpi_2 = 0$  to  $\varpi_1 = \varpi_2 = 0.1$ . The solid and dashed curves represent the outage behaviors of  $x_1$  and  $x_2$  with ipSIC/pSIC, respectively. As can be seen that when the impact level of IS is set to be  $\varpi_1 = \varpi_2 = 0$ , there is no IS between  $A_1$  and  $A_2$  at the relay, which can be viewed as a benchmark. Additionally, one can observed that with the impact levels of IS increasing, the outage performance of TWR-NOMA system degrades significantly. Hence it is crucial to hunt for efficient strategies for suppressing the effect of interference between antennas. Fig. 3 plots the outage probability versus SNR with different values of residual IS from  $-20$  dB to  $0$  dB. It can be seen that the different values of residual IS affects the performance

## V. CONCLUSION

This paper has investigated the application of TWR to NOMA systems, in which two pairs of users can exchange their information between each other by the virtue of a relay node. The performance of TWR-NOMA has been characterized in terms of outage probability and ergodic rate for both ipSIC and pSIC. Furthermore, the closed-form expressions of outage probability for the NOMA users' signals have been derived. Owing to the impact of IS at relay, there were the error floors for TWR-NOMA with ipSIC/pSIC in high SNR regimes and zero diversity orders were obtained. Based on the analytical results, it was shown that the performance of TWR-NOMA with ipSIC/pSIC outperforms TWR-OMA in the low SNR regime.

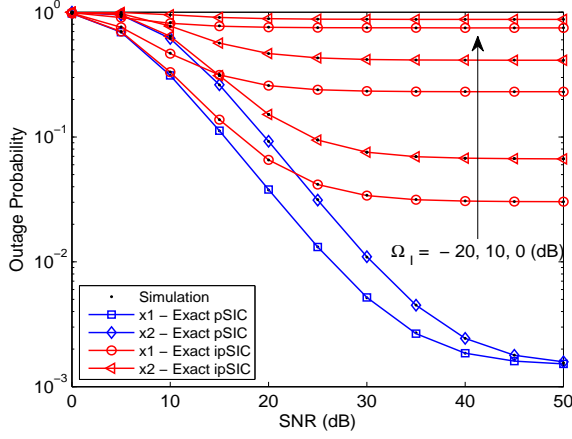


Fig. 3: Outage probability versus the transmit SNR, with  $\varpi_1 = \varpi_2 = 0$ .

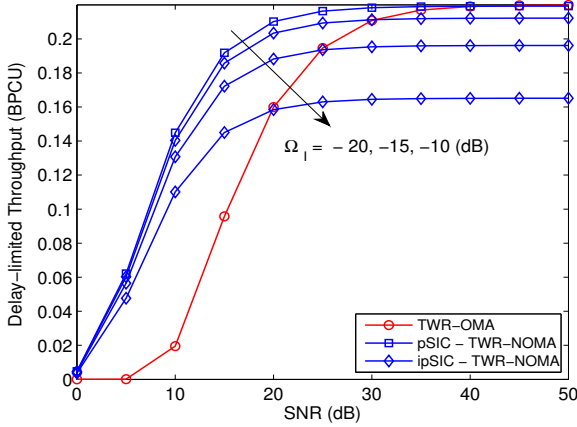


Fig. 4: System throughput in delay-limited transmission mode versus SNR with ipSIC/pSIC,  $\varpi_1 = \varpi_2 = 0.01$ .

of ipSIC seriously. Similarly, as the values of residual IS increases, the preponderance of ipSIC is inexistent. When  $\Omega_I = 0$  dB, the outage probability of  $x_1$  and  $x_2$  will be in close proximity to one. Therefore, it is important to design effective SIC schemes for TWR-NOMA.

Fig. 4 plots system throughput versus SNR in delay-limited transmission mode for TWR-NOMA with different values of residual IS from  $-20$  dB to  $-10$  dB. The blue solid curves represent throughput for TWR-NOMA with both pSIC and ipSIC, which can be obtained from (19). One can observe that TWR-NOMA is capable of achieving a higher throughput compared to TWR-OMA in the low SNR regime, since it has a lower outage probability. Moreover, the figure confirms that TWR-NOMA converges to the throughput ceiling in high SNR regimes. It is worth noting that ipSIC considered for TWR-NOMA will further degrade throughput with the values of residual IS becomes larger in high SNR regimes.

## APPENDIX A: PROOF OF THEOREM 1

Substituting (3), (5) and (6) into (8), the outage probability of  $x_l$  can be further given by

$$\begin{aligned}
 P_{x_l}^{ipSIC} &= 1 \\
 &- \Pr \left( \underbrace{\frac{\rho|h_l|^2 a_l}{\rho|h_t|^2 a_t + \rho\varpi_1(|h_k|^2 a_k + |h_r|^2 a_r) + 1}}_{J_1} > \gamma_{th_l} \right) \\
 &\times \Pr \left( \underbrace{\frac{\rho|h_k|^2 b_t}{\rho|h_k|^2 b_l + \rho\varpi_2|h_k|^2 + 1}}_{J_2} > \gamma_{th_t}, \right. \\
 &\quad \left. \frac{\rho|h_k|^2 b_l}{\varepsilon\rho|g|^2 + \rho\varpi_2|h_k|^2 + 1} > \gamma_{th_l} \right), \quad (A.1)
 \end{aligned}$$

where  $\varepsilon = 1$ .

To calculate the probability  $J_1$  in (A.1), let  $Z = \rho a_t |h_t|^2 + \rho\varpi_1 a_k |h_k|^2 + \rho\varpi_1 a_r |h_r|^2$ . We first calculate the PDF of  $Z$  and then give the process derived of  $J_1$ . As is known,  $|h_i|^2$  follows the exponential distribution with the means  $\Omega_i$ ,  $i \in (1, 2, 3, 4)$ . Furthermore, we denote that  $Z_1 = \rho a_t |h_t|^2$ ,  $Z_2 = \rho\varpi_1 a_k |h_k|^2$  and  $Z_3 = \rho\varpi_1 a_r |h_r|^2$  are also independent exponentially distributed random variables (RVs) with means  $\lambda_1 = \frac{1}{\rho a_t \Omega_t}$ ,  $\lambda_2 = \frac{1}{\rho\varpi_1 a_k \Omega_k}$  and  $\lambda_3 = \frac{1}{\rho\varpi_1 a_r \Omega_r}$ , respectively. Based on [18], for the independent non-identical distributed (i.n.d) fading scenario, the PDF of  $Z$  can be given by

$$f_Z(z) = \prod_{i=1}^3 \lambda_i (\Phi_1 e^{-\lambda_1 z} - \Phi_2 e^{-\lambda_2 z} + \Phi_3 e^{-\lambda_3 z}), \quad (A.2)$$

where  $\Phi_1 = \frac{1}{(\lambda_2 - \lambda_1)(\lambda_3 - \lambda_1)}$ ,  $\Phi_2 = \frac{1}{(\lambda_3 - \lambda_2)(\lambda_2 - \lambda_1)}$  and  $\Phi_3 = \frac{1}{(\lambda_3 - \lambda_1)(\lambda_3 - \lambda_2)}$ .

According to the above explanations,  $J_1$  is calculated as follows:

$$J_1 = \Pr \left( |h_l|^2 > (Z + 1) \beta_l \right) = \int_0^\infty f_Z(z) e^{-\frac{(z+1)\beta_l}{\Omega_l}} dz. \quad (A.3)$$

Substituting (A.2) into (A.3) and after some algebraic manipulations,  $J_1$  is given by

$$J_1 = e^{-\frac{\beta_l}{\Omega_l}} \prod_{i=1}^3 \lambda_i \left( \frac{\Phi_1 \Omega_l}{\Omega_l \lambda_1 + \beta_l} - \frac{\Phi_2 \Omega_l}{\Omega_l \lambda_2 + \beta_l} + \frac{\Phi_3 \Omega_l}{\Omega_l \lambda_3 + \beta_l} \right), \quad (\text{A.4})$$

where  $\beta_l = \frac{\gamma_{th_l}}{\rho a_l}$ .

$J_2$  can be further calculated as follows:

$$\begin{aligned} J_2 &= \Pr \left( |h_k|^2 > \max(\tau_l, \xi_t) \triangleq \theta_l, |g|^2 < \frac{|h_k|^2 - \tau_l}{\varepsilon \rho \tau_l} \right) \\ &= \int_{\theta}^{\infty} \frac{1}{\Omega_k} \left( e^{-\frac{y}{\Omega_k}} - e^{-\frac{y-\tau_l}{\varepsilon \tau_l \rho \Omega_l} - \frac{y}{\Omega_k}} \right) dy \\ &= e^{-\frac{\theta_l}{\Omega_k}} - \frac{\tau_l \varepsilon \rho \Omega_l}{\Omega_k + \varepsilon \rho \tau_l \Omega_l} e^{-\frac{\theta_l (\Omega_k + \varepsilon \rho \tau_l \Omega_l)}{\tau_l \varepsilon \rho \Omega_l \Omega_k} + \frac{1}{\varepsilon \rho \Omega_l}}, \quad (\text{A.5}) \end{aligned}$$

where  $\xi_t = \frac{\gamma_{th_t}}{\rho(b_l - b_l \gamma_{th_t} - \varpi_2 \gamma_{th_t})}$  with  $b_l > (b_l + \varpi_2) \gamma_{th_t}$ ,  $\tau_l = \frac{\gamma_{th_l}}{\rho(b_l - \varpi_2 \gamma_{th_l})}$  with  $b_l > \varpi_2 \gamma_{th_l}$ . Combining (A.4) and (A.5), we can obtain (9). The proof is complete.

## APPENDIX B: PROOF OF THEOREM 2

Substituting (3), (4), (6) and (7) into (11), the outage probability of  $x_t$  is rewritten as

$$\begin{aligned} P_{x_t}^{ipSIC} &= 1 \\ &- \Pr \left( \frac{\rho |h_t|^2 a_t}{\varepsilon \rho |g|^2 + \rho \varpi_1 (|h_k|^2 a_k + |h_r|^2 a_r) + 1} > \gamma_{th_t}, \right. \\ &\quad \left. \frac{\rho |h_l|^2 a_l}{\rho |h_t|^2 a_t + \rho \varpi_1 (|h_k|^2 a_k + |h_r|^2 a_r) + 1} > \gamma_{th_l} \right) \\ &\quad \underbrace{\hspace{10em}}_{\Theta_1} \\ &\times \Pr \left( \frac{\rho |h_l|^2 b_t}{\rho |h_k|^2 b_l + \rho \varpi_2 |h_k|^2 + 1} > \gamma_{th_t} \right) \\ &\quad \underbrace{\hspace{10em}}_{\Theta_2} \\ &\times \Pr \left( \frac{\rho |h_r|^2 b_t}{\rho |h_r|^2 b_l + \rho \varpi_2 |h_r|^2 + 1} > \gamma_{th_t} \right), \quad (\text{B.1}) \\ &\quad \underbrace{\hspace{10em}}_{\Theta_3} \end{aligned}$$

where  $\varpi_1 = \varpi_2 \in [0, 1]$  and  $\varepsilon = 1$ .

Similar to (A.2), let  $Z' = \rho \varpi_1 a_k |h_k|^2 + \rho \varpi_1 a_r |h_r|^2$ , the PDF of  $Z'$  is given by

$$f_{Z'}(z') = \prod_{i=1}^2 \lambda'_i \left( \frac{e^{-\lambda'_1 z'}}{(\lambda'_2 - \lambda'_1)} - \frac{e^{-\lambda'_2 z'}}{(\lambda'_2 - \lambda'_1)} \right), \quad (\text{B.2})$$

where  $\lambda'_1 = \frac{1}{\rho \varpi_1 a_k \Omega_k}$  and  $\lambda'_2 = \frac{1}{\rho \varpi_1 a_r \Omega_r}$ .

After some variable substitutions and manipulations,

$$\begin{aligned} \Theta_1 &= \Pr \left( |h_t|^2 > \beta_t \left( \varepsilon \rho |g|^2 + Z' + 1 \right), \right. \\ &\quad \left. |h_l|^2 > \beta_l \left( \rho |h_t|^2 a_t + Z' + 1 \right) \right) \\ &= \frac{1}{\varphi_t \Omega_t (1 + \varepsilon \rho \beta_t \varphi_t \Omega_l)} e^{-\frac{\beta_l}{\Omega_l} - \beta_t \varphi_t} \\ &\quad \times \int_0^{\infty} f_{Z'}(z') e^{-\frac{(\beta_l + \beta_t \Omega_l \varphi_t) z'}{\Omega_l}} dx, \quad (\text{B.3}) \end{aligned}$$

where  $\beta_t = \frac{\gamma_{th_t}}{\rho a_t}$  and  $\varphi_t = \frac{\Omega_l + \rho \beta_l a_t \Omega_l}{\Omega_l \Omega_t}$ .

Substituting (B.2) into (B.3),  $\Theta_1$  can be given by

$$\begin{aligned} \Theta_1 &= \frac{e^{-\frac{\beta_l}{\Omega_l} - \beta_t \varphi_t}}{\varphi_t \Omega_t (1 + \beta_t \varepsilon \rho \varphi_t \Omega_l) (\lambda'_2 - \lambda'_1)} \\ &\times \prod_{i=1}^2 \lambda'_i \left( \frac{\Omega_l}{\beta_l + \beta_t \Omega_l \varphi_t + \Omega_l \lambda'_1} - \frac{\Omega_l}{\beta_l + \beta_t \Omega_l \varphi_t + \Omega_l \lambda'_2} \right). \quad (\text{B.4}) \end{aligned}$$

$\Theta_2$  and  $\Theta_3$  can be easily calculated

$$\Theta_2 = \Pr \left( |h_k|^2 > \xi_t \right) = e^{-\frac{\xi_t}{\Omega_k}}, \quad (\text{B.5})$$

and

$$\Theta_3 = \Pr \left( |h_r|^2 > \xi_t \right) = e^{-\frac{\xi_t}{\Omega_r}}, \quad (\text{B.6})$$

respectively, where  $\xi_t = \frac{\gamma_{th_t}}{\rho(b_l - b_l \gamma_{th_t} - \varpi_2 \gamma_{th_t})}$  with  $b_l > (b_l + \varpi_2) \gamma_{th_t}$ .

Finally, combining (B.4), (B.5) and (B.6), we can obtain (12). The proof is complete.

## REFERENCES

- [1] Y. Liu, Z. Qin, M. ElKashlan, Z. Ding, A. Nallanathan, and L. Hanzo, "Nonorthogonal multiple access for 5G and beyond," *Proceedings of the IEEE*, vol. 105, no. 12, pp. 2347–2381, Dec. 2017.
- [2] Z. Ding, Y. Liu, J. Choi, Q. Sun, M. ElKashlan, C. L. I, and H. V. Poor, "Application of non-orthogonal multiple access in LTE and 5G networks," *IEEE Commun. Mag.*, vol. 55, no. 2, pp. 185–191, Feb. 2017.
- [3] S. M. R. Islam, N. Avazov, O. A. Dobre, and K. s. Kwak, "Power-domain non-orthogonal multiple access (noma) in 5G systems: Potentials and challenges," *IEEE Commun. Surveys. Tutorials*, vol. 19, no. 2, pp. 721–742, Sec. 2017.
- [4] Y. Cai, Z. Qin, F. Cui, G. Y. Li, and J. A. McCann, "Modulation and multiple access for 5G networks," *IEEE Commun. Surveys. Tutorials*, vol. PP, no. 99, pp. 1–1, 2017.
- [5] T. M. Cover and J. A. Thomas, *Elements of information theory*, 6th ed., Wiley and Sons, New York, 1991.
- [6] Z. Ding, M. Peng, and H. V. Poor, "Cooperative non-orthogonal multiple access in 5G systems," *IEEE Commun. Lett.*, vol. 19, no. 8, pp. 1462–1465, Aug. 2015.
- [7] Y. Liu, Z. Ding, M. ElKashlan, and H. V. Poor, "Cooperative non-orthogonal multiple access with simultaneous wireless information and power transfer," *IEEE J. Sel. Areas Commun.*, vol. 34, no. 4, pp. 938–953, Apr. 2016.
- [8] J. Men, J. Ge, and C. Zhang, "Performance analysis of non-orthogonal multiple access for relaying networks over Nakagami- $m$  fading channels," *IEEE Trans. Veh. Technol.*, to appear in 2016.
- [9] X. Yue, Y. Liu, S. Kang, A. Nallanathan, and Z. Ding, "Outage performance of full/half-duplex user relaying in NOMA systems," in *IEEE Proc. of International Commun. Conf. (ICC)*, Paris, FRA, May. 2017, pp. 1–6.
- [10] C. E. Shannon, "Two-way communication channels," in *Proc. 4th Berkeley Symp. Math. Stat and Prob.*, vol. 1, pp. 611–644, 1961.

- [11] A. Hyadi, M. Benjillali, and M. S. Alouini, "Outage performance of decode-and-forward in two-way relaying with outdated CSI," *IEEE Trans. Veh. Technol.*, vol. 64, no. 12, pp. 5940–5947, Dec. 2015.
- [12] C. Li, B. Xia, S. Shao, Z. Chen, and Y. Tang, "Multi-user scheduling of the full-duplex enabled two-way relay systems," *IEEE Trans. Wireless Commun.*, vol. 16, no. 2, pp. 1094–1106, Feb. 2017.
- [13] Z. Ding, Z. Yang, P. Fan, and H. V. Poor, "On the performance of non-orthogonal multiple access in 5G systems with randomly deployed users," *IEEE Signal Process. Lett.*, vol. 21, no. 12, pp. 1501–1505, Dec. 2014.
- [14] Y. Liu, Z. Qin, M. ElKashlan, A. Nallanathan, and J. A. McCann, "Non-orthogonal multiple access in large-scale heterogeneous networks," *IEEE J. Sel. Areas Commun.*, vol. 35, no. 12, pp. 2667–2680, Dec. 2017.
- [15] M. F. Kader, M. B. Shahab, and S. Y. Shin, "Exploiting non-orthogonal multiple access in cooperative relay sharing," *IEEE Commun. Lett.*, to appear in 2017.
- [16] Y. Liu, Z. Ding, M. ElKashlan, and J. Yuan, "Non-orthogonal multiple access in large-scale underlay cognitive radio networks," *IEEE Trans. Veh. Technol.*, vol. 65, no. 12, pp. 10 152–10 157, Dec. 2016.
- [17] Y. Liu, Z. Qin, M. ElKashlan, Y. Gao, and L. Hanzo, "Enhancing the physical layer security of non-orthogonal multiple access in large-scale networks," *IEEE Trans. Wireless Commun.*, vol. 16, no. 3, pp. 1656–1672, Mar. 2017.
- [18] S. Nadarajah, "A review of results on sums of random variables," *Acta Appl. Math.*, vol. 103, no. 2, pp. 131–141, Sep. 2008.